

## Goos-Hänchen shifts in spin-orbit-coupled cold atoms

Lu Zhou,<sup>1</sup> Jie-Li Qin,<sup>1</sup> Zhihao Lan,<sup>2,\*</sup> Guangjiong Dong,<sup>1</sup> and Weiping Zhang<sup>1,†</sup>

<sup>1</sup>*Department of Physics, State Key Laboratory of Precision Spectroscopy, Quantum Institute for Light and Atoms, East China Normal University, Shanghai 200062, China*

<sup>2</sup>*Mathematical Sciences, University of Southampton, Southampton, SO17 1BJ, United Kingdom*

(Received 19 October 2014; published 17 March 2015)

We consider a matter wave packet of cold atom gas impinging upon a step potential created by an optical light field. In the presence of spin-orbit coupling, the atomic eigenstates contain two types of evanescent states, one of which is an ordinary evanescent state with a pure imaginary wave vector while the other possesses a complex wave vector and is recognized as an oscillating evanescent state. We show that the presence and interplay of these two types of evanescent states can give rise to two different mechanisms for total internal reflection, and thus lead to an unusual Goos-Hänchen (GH) effect. As a result, not only large positive but also large negative GH shifts can be observed in the reflected atomic beam. The dependence of the GH shift on the incident angle, energy, and height of the step potential is studied numerically.

DOI: [10.1103/PhysRevA.91.031603](https://doi.org/10.1103/PhysRevA.91.031603)

PACS number(s): 03.75.-b, 42.25.Bs, 42.50.Gy

The Goos-Hänchen (GH) effect was first discovered in 1947 [1] as an optical phenomenon in which a light beam incident upon the interface of two media can experience a lateral shift under the condition of total internal reflection (TIR). The origin of this lateral shift is rooted in the fact that the incident beam is composed of different plane-wave components with finite transverse distribution, which will experience different phase shifts during TIR. So the key physics inherent in the GH effect is wave interference, and in this sense it can also be generated with a matter wave. As a matter of fact, a GH shift in graphene [2], neutron [3], and even atom optics [4] has been predicted.

Among these, the electronic analog of the GH effect has been carefully studied [5]. Compared to an electromagnetic wave, an electron provides an extra degree of freedom for tuning the GH effect. For example, the effective electron mass can be tuned from positive to negative [6], therefore a negative GH shift can be observed. In graphene [2,7], for massless electrons in the ultrarelativistic limit, it was found that the GH effect becomes dependent on the spin degree of freedom. However, the electronic GH shift is about an order of the electron de Broglie wavelength (on the scale of a nanometer), which impedes its direct observation in experiments. Recent years have witnessed a rapid advancement in laser cooling and trapping technology, which made ultracold atoms with a relatively long de Broglie's wavelength available. As such, phenomena originally predicted for electrons in the ultrarelativistic limit, such as *Zitterbewegung* [8] and Klein tunneling [9], have been successfully observed in experiments with cold atoms [10,11], thus making cold atom systems appealing for the study of the GH and relativistic effects [12].

Furthermore, recent experimental progress has also implemented spin-orbit (SO) coupling in ultracold atomic gas by dressing cold atoms with lasers of a special configuration [13]. In electronic systems, SO coupling can originate from the

interaction between the intrinsic electronic spin and the magnetic field induced by its movement. It connects the electronic spin to its orbital motion and thus the electron transport becomes spin dependent. In the presence of SO coupling, apart from the normal evanescent states, there exist oscillating evanescent states [14], in which the matter wave propagates with a complex longitudinal wave vector. The role of the SO interaction and evanescent states on the tunneling dynamics of electrons has been studied previously [14,15]. However, the role of these evanescent states on the TIR and thus the GH effect still needs to be explored. As we will show in the following, the presence and interplay of these two types of evanescent states can give rise to two different mechanisms for TIR, and thus lead to an unusual GH effect.

The Rashba SO coupling can be generated in neutral cold atoms with a tripod scheme [16–18], in which the atomic electronic energy-level structure is composed of an excited state  $|0\rangle$  and three degenerate hyperfine ground states  $|1\rangle$ ,  $|2\rangle$ , and  $|3\rangle$ . The ground state  $|j\rangle$  ( $j = 1, 2, 3$ ) is coupled to  $|0\rangle$  via a laser field with Rabi frequency  $\Omega_j$ . By appropriately designing the laser configurations [17,18], the atom-laser coupling system supports two degenerate dark states, which are also the ground states of the system. In the subspace spanned by the dark states, the effective Hamiltonian can be written as

$$H = \frac{\hbar^2 \mathbf{k}^2}{2m} + \hbar\alpha(k_x\sigma_y - k_y\sigma_x) + V(x), \quad (1)$$

with  $\mathbf{k}^2 = k_x^2 + k_y^2$ ,  $\alpha$  is the Rashba SO coupling strength,  $\sigma_x = [0, 1; 1, 0]$ ,  $\sigma_y = [0, -i; i, 0]$  are the Pauli matrices acting on the two spin components, and the scattering potential is described by  $V(x) = V_0\Theta(x)$ , where  $\Theta(x)$  is the Heaviside step function. Such a step potential can be created via a super-Gaussian laser beam with a large-enough order [19] and width compared to the atomic de Broglie wavelength.

In the case where  $V(x) = V_0$  is a constant potential, the eigenfunctions of Hamiltonian (1) split into two branches and can generally be expressed as

$$\phi_{\mathbf{k}}^{\pm} = C e^{i(k_x x + k_y y)} \begin{pmatrix} -2a(k_y + ik_x) \\ E_{\mathbf{k}}^{\pm} - V_0 - \mathbf{k}^2 \end{pmatrix}, \quad (2)$$

\*Present address: School of Physics and Astronomy, University of Nottingham, Nottingham NG7 2RD, United Kingdom; zhihao.lan@nottingham.ac.uk

†wpzhang@phy.ecnu.edu.cn

with  $C$  the normalization constant and  $a = m\alpha/\hbar$ .  $E_{\mathbf{k}}^{\pm}$  is the corresponding eigenenergy (scaled by  $\hbar^2/2m$ ) satisfying the relation

$$(\mathbf{k}^2 + V_0 - E_{\mathbf{k}})^2 - 4a^2\mathbf{k}^2 = 0, \quad (3)$$

from which we can get the energy spectrum  $E_{\mathbf{k}} = k^2 \pm 2ak + V_0$  or the modulus of the wave vector  $k = \mp a + \sqrt{a^2 + E_{\mathbf{k}} - V_0}$ .

In the situation considered here, the system is left free along the  $y$  direction and is semi-infinite in the  $x$  direction, thus  $k_y$  is real and  $k_x$  is generally complex. As those had been illustrated in Ref. [14], the eigenfunctions of the system can be grouped into three categories according to their properties: propagating states with  $k_x$  real, evanescent states (only existing near the boundary of the system and propagating along it) with  $k_x = i\kappa$  (requiring  $|\kappa| < |k_y|$ ) and oscillating evanescent states with  $k_x = K'_x + iK''_x$ , in which  $K'_x, K''_x$  satisfy  $K_x'^2 K_x''^2 = a^2(V_0 - E - a^2)$  and  $K_x'^2 - K_x''^2 = 2a^2 + E - V_0 - k_y^2$ . It is clear that in order for the oscillating evanescent states to exist, the condition of  $V_0 > a^2 + E$  needs to be satisfied.

In order to better understand the properties of these eigenstates, we plot in Fig. 1 the energy spectra ( $E_{\mathbf{k}} - V_0$ ) as a function of  $|k_x|$  for two typical values of  $k_y$ , which exhibit different structures depending on the value of  $k_y$ . For both cases, the two branches of propagating states are separated by a gap of  $4a|k_y|$  at  $|k_x| = 0$ . When  $|k_y| < a$ ,  $|k_x| = \sqrt{a^2 - k_y^2}$  is the energy minimum of the lower propagating branch and the dispersion curve of the evanescent states forms a lobe with its tip located at  $|k_x| = |k_y|$ , which intersects with the energy spectra of propagating states at  $|k_x| = 0$ . For  $|k_y| > a$ ,  $|k_x| = 0$  becomes the energy minimum of the lower propagating branch, which intersects with the evanescent lobe at some finite  $|k_x|$  besides  $|k_x| = 0$ . The oscillating evanescent states possess minimum energies among these three types of solutions for both cases, and they are linked to the energy minimum of the

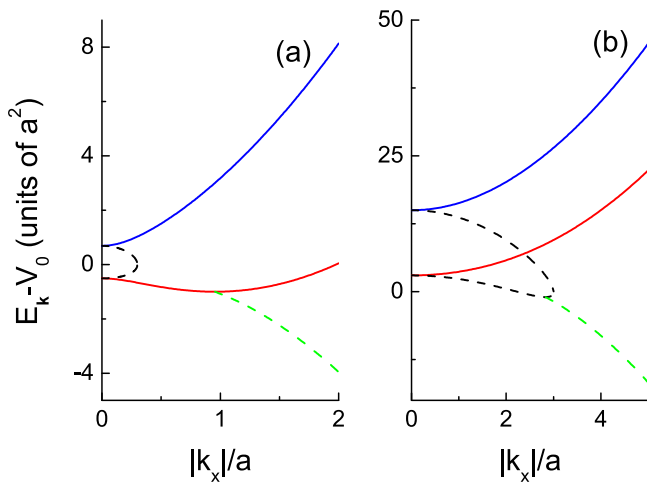


FIG. 1. (Color online) Energy spectra of the different states described by  $E_{\mathbf{k}} = k^2 \pm 2ak + V_0$ . The solid (blue and red) lines correspond to the up and down branches of the propagating states. The black dashed line represents the evanescent states while the green (light) dashed line is for the oscillating evanescent states. The parameters are set as (a)  $k_y = 0.3a$  and (b)  $k_y = 3a$ .

lower propagating branch for  $|k_y| < a$  and the evanescent lobe for  $|k_y| > a$ .

The presence of two different types of evanescent states provides different possibilities for TIR and could have a crucial effect on the resulting GH shift. It would be convenient to discuss the conditions for TIR to happen before we move on to the calculations and discussions of the GH shift. First, the energy spectra in Fig. 1 indicate that, in order for TIR to take place, the incident atomic beam should be prepared in the lower dispersion branch of the propagating states or the “outer circles” on the left in Fig. 2. This is because any propagating states prepared in the upper branch (or “inner circle”) will always lead to double reflection [20] instead of TIR. Second, in the normal case without SO coupling, there will be a pure evanescent wave along the inner boundary of the step potential when TIR takes place. The GH shift in this case can then be understood as to account for the penetration of the evanescent

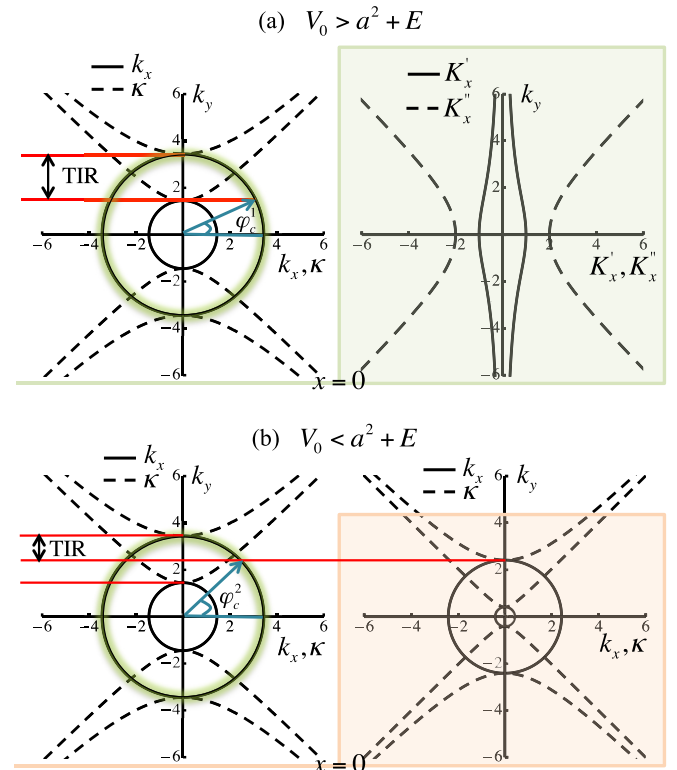


FIG. 2. (Color online) Schematic to illustrate the two different mechanisms for TIR when the incident beam is prepared in the  $k = a + \sqrt{a^2 + E}$  branch of the propagating states (outer circles in the left). The different eigenstates in (a) and (b) are plotted with  $E = 5a^2$ ,  $V_0 = 10a^2$  and  $E = 5a^2$ ,  $V_0 = 4a^2$ , respectively, however, the figure is for illustrative purposes only. In (a), where  $V_0 > a^2 + E$  such that only oscillating evanescent states exist inside the step potential, the range of  $k_y$  that gives TIR as marked by the arrows is determined by the incident energy  $E$  of the beam only. In (b), where  $V_0 < a^2 + E$  and consequently no oscillating evanescent state exists inside the step potential, the TIR happens only when evanescent states are available at both sides of the potential. As a result, the range of  $k_y$  that gives TIR has an additional constraint from the potential compared with the case in (a) and the critical angle for TIR to happen crucially depends on the height of the potential.

field to the other side of the interface and, as such, the GH shift should be positive. The different physics inherent in the present case with SO coupling can be understood as there are two different mechanisms needed for TIR to take place.

(i) When  $V_0 > a^2 + E$ , the only available states inside the step potential are oscillating evanescent ones. So the TIR happens when one of the reflected beams at the  $x < 0$  side is evanescent [see the range of  $k_y$  marked by the arrows in Fig. 2(a)], the lower bound of which defines the critical incident angle  $\varphi_c^1$  of the TIR,

$$\varphi_c^1 = \sin^{-1} \frac{\sqrt{E + a^2} - a}{\sqrt{E + a^2} + a}, \quad (4)$$

which is independent of the height of the step potential. The available oscillating evanescent states inside the step potential are composed of two counterpropagating ones [ $\pm K'_x$ —see the right of Fig. 2(a)], one of which penetrates along the potential boundary and gives rise to an evanescent wave on the outer boundary of the step potential. This accounts for the creation of negative GH shifts.

(ii) When  $V_0 < a^2 + E$  such that no oscillating evanescent state exists inside the step potential, the TIR occurs only when evanescent states are available at both sides of the potential. Thus, apart from the marked range of  $k_y$  as in the case of  $V_0 > a^2 + E$ , there is an extra constraint from the potential side. The lower bound of the overlapped range as marked in Fig. 2(b) defines the critical incident angle  $\varphi_c^2$  for the TIR to happen in this case,

$$\varphi_c^2 = \sin^{-1} \frac{\sqrt{E - V_0 + a^2} + a}{\sqrt{E + a^2} + a}, \quad (5)$$

and in this case the critical angle shows a crucial dependence on the height of the step potential.

After the discussion of the two different mechanisms needed for TIR to occur, we now proceed to the calculations and discussions of the resulting GH shifts. The atoms are initially prepared in the  $k = a + \sqrt{a^2 + E}$  branch of the propagating states with energy  $E$  and, incident upon the step potential from  $x < 0$ , the wave function reads

$$\Psi_{\text{in}} = \int dk_y f(k_y - k_{y0}) e^{i(k_x x + k_y y)} \begin{pmatrix} -e^{-i\varphi(k_y)/2} \\ i e^{i\varphi(k_y)/2} \end{pmatrix}, \quad (6)$$

$$\Psi_t = \int dk_y f(k_y - k_{y0}) e^{-K'_x x + i k_y y} \left[ b_1(k_y) \begin{pmatrix} a \frac{iK'_x - K''_x + k_y}{a^2 + iK'_x K''_x} \\ 1 \end{pmatrix} e^{iK'_x x} + b_2(k_y) e^{-iK'_x x} \begin{pmatrix} a \frac{-iK'_x - K''_x + k_y}{a^2 - iK'_x K''_x} \\ 1 \end{pmatrix} \right], \quad (10)$$

in which  $K'_x$  and  $K''_x$  are positive real and  $b_{1(2)}$  are the transmission amplitudes.

By integrating the Schrödinger equation  $H\Psi(x) = E\Psi(x)$  over the interval expanded around the interface  $x = 0$ , we get

$$\Psi_{\text{in}}|_{x=0} + \Psi_r|_{x=0} + \Psi_e|_{x=0} = \Psi_t|_{x=0}, \quad \frac{\partial \Psi_{\text{in}}}{\partial x} \Big|_{x=0} + \frac{\partial \Psi_r}{\partial x} \Big|_{x=0} + \frac{\partial \Psi_e}{\partial x} \Big|_{x=0} = \frac{\partial \Psi_t}{\partial x} \Big|_{x=0}, \quad (11)$$

From Eqs. (11), the scattering index  $\{r, s, b_1, b_2\}$  can be found to satisfy the following matrix equation,

$$\mathcal{M} \begin{pmatrix} r \\ s \\ b_1 \\ b_2 \end{pmatrix} = \begin{pmatrix} e^{-i\varphi/2} \\ -i e^{i\varphi/2} \\ i k_x e^{-i\varphi/2} \\ k_x e^{i\varphi/2} \end{pmatrix}, \quad (12)$$

in which the distribution function  $f(k_y - k_{y0})$  describes that the incident atomic beam has a narrow angular distribution centering at  $k_y = k_{y0}$  with incident angle  $\varphi(k_y) = \arg(k_x + i k_y)$ . We can then expand  $\varphi(k_y)$  around  $k_y = k_{y0}$  and as such  $\varphi(k_y) \simeq \varphi(k_{y0}) + \varphi'(k_{y0})k_y$ . By using the Fourier transform shift theorem, i.e., a linear phase shift in the wave-vector domain introduces a translation in the space domain, the center of the incident atomic beam for the two spin components at  $x = 0$  will locate at  $y_{\pm}^{\text{in}} = \pm \varphi'(k_{y0})/2$ , respectively.

Under the condition of TIR, from Fig. 2 we know that the reflected wave is a linear superposition of two waves: One is the reflected propagating wave,

$$\Psi_r = \int dk_y f(k_y - k_{y0}) e^{i(-k_x x + k_y y)} r(k_y) \begin{pmatrix} i e^{i\varphi(k_y)/2} \\ -e^{-i\varphi(k_y)/2} \end{pmatrix}, \quad (7)$$

which is obtained from Eq. (6) by replacing  $k_x \rightarrow -k_x$ ,  $\varphi \rightarrow \pi - \varphi$ , and  $r(k_y) = |r(k_y)| e^{i\phi(k_y)}$  is the reflection amplitude. The other wave on the incident side is an evanescent one,

$$\Psi_e = \int dk_y f(k_y - k_{y0}) e^{\kappa x + i k_y y} s(k_y) \begin{pmatrix} -\frac{2a(\kappa + k_y)}{E - k_y^2 + \kappa^2} \\ 1 \end{pmatrix}, \quad (8)$$

in which  $s$  is the reflection amplitude of the evanescent wave with  $\kappa > 0$ . In the case of TIR,  $|r(k_y)| = 1$  becomes independent of  $k_y$ , then at the interface  $x = 0$  the center of the two reflected atomic components will be at  $y_{\pm}^r = -\phi'(k_{y0}) \mp \varphi'(k_{y0})/2$ . Combining the expressions of  $y_{\pm}^r$  and  $y_{\pm}^{\text{in}}$ , the atomic beam will experience a lateral shift upon TIR:  $\sigma_{\pm} = y_{\pm}^r - y_{\pm}^{\text{in}} = -\phi'(k_{y0}) \mp \varphi'(k_{y0})$  and the average shift

$$\sigma = (\sigma_+ + \sigma_-)/2 = -\phi'(k_{y0}) \quad (9)$$

is recognized as the GH shift.

As we have discussed above, under the condition of TIR the states in the step potential can be either oscillating evanescent states ( $V_0 > a^2 + E$ ) or evanescent states ( $V_0 < a^2 + E$ ). The theoretical derivations of the reflection amplitudes in the two cases are similar, i.e., first write down the wave function inside the step potential and then match the wave function using the boundary conditions at  $x = 0$ . In the following, we will focus on the derivation when the oscillating evanescent states are the only available ones [21], such that the waves in the step potential have the following form,

with

$$\mathcal{M} = \begin{pmatrix} ie^{i\varphi/2} & -2a \frac{\kappa+k_y}{E-k_y^2+\kappa^2} & -a \frac{iK'_x-K''_x+k_y}{a^2+iK'_xK''_x} & -a \frac{-iK'_x-K''_x+k_y}{a^2-iK'_xK''_x} \\ -e^{-i\varphi/2} & 1 & -1 & -1 \\ k_x e^{i\varphi/2} & -2a\kappa \frac{\kappa+k_y}{E-k_y^2+\kappa^2} & -a(iK'_x-K''_x) \frac{iK'_x-K''_x+k_y}{a^2+iK'_xK''_x} & a(iK'_x+K''_x) \frac{-iK'_x-K''_x+k_y}{a^2-iK'_xK''_x} \\ ik_x e^{-i\varphi/2} & \kappa & -iK'_x+K''_x & iK'_x+K''_x \end{pmatrix}, \quad (13)$$

from which the reflection amplitude  $r$  can be derived straightforwardly as

$$r = \frac{e^{-i\varphi/2}A + ie^{i\varphi/2}B + ik_x e^{-i\varphi/2}C - k_x e^{i\varphi/2}D}{ie^{i\varphi/2}A + e^{-i\varphi/2}B + k_x e^{i\varphi/2}C - ik_x e^{-i\varphi/2}D}, \quad (14)$$

where  $A, B, C, D$  are minors of the first column entries of matrix  $\mathcal{M}$ .

By calculating the phase shift inherent in the reflection amplitude  $r = e^{i\phi(k_y)}$  according to Eq. (9) under the condition of TIR, the GH shift can be derived and the results are shown in Figs. 3 and 4. The GH shift is scaled in units of  $a^{-1}$ , which is the wavelength of the light field used to create the SO coupling and is on the order of several hundred nanometers. This is much larger than the electronic de Broglie wavelength and could be easily observed in cold atom experiments. From Fig. 3 one can see that when the incident angle exceeds the critical angle ( $0.0076\pi$ ), TIR will take place. This critical angle is independent of the step potential height  $V_0$ , resulting from the fact that  $V_0 > E + a^2$ . From Fig. 3 one can also observe the appearance of a negative GH shift. With an increase of the incident energy  $E$ , the GH shift will gradually become positive.

The dependence of the GH shifts on the height of the potential  $V_0$  and the incident energy  $E$  are shown in Fig. 4. Figure 4(a) verifies that TIR occurs only when Eq. (5) is satisfied. For example, when the incident energy is  $E = 5a^2$ , according to Eq. (5), for incident angles of  $\pi/6$  and  $\pi/3$ , the critical heights of the step potential for the TIR to occur are  $5.47a^2$  and  $2.05a^2$ , respectively, which show good agreement with the numerics in Fig. 4(a). On the other hand, Fig. 4(b) indicates that a negative GH shift can only be observed for very small incident energy and the TIR will take place in

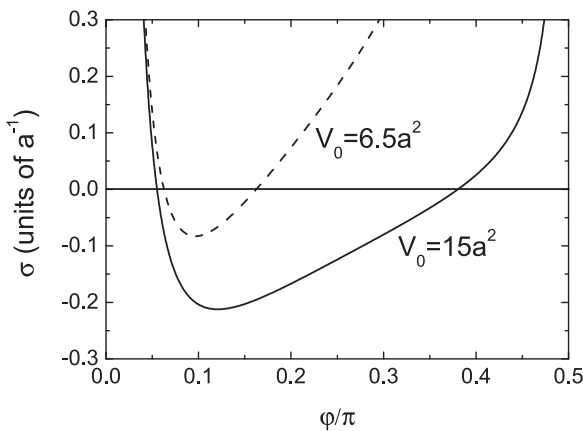


FIG. 3. The GH shift  $\sigma$  vs the incident angle  $\varphi$  for  $E = 0.1a^2$  and  $V_0 = 15a^2$  (solid line),  $V_0 = 6.5a^2$  (dashed line).

a larger energy interval with a larger incident angle. Again, the theoretical critical energies for TIR to happen according to Eqs. (4) and (5) with incident angles of  $\pi/12$ ,  $\pi/6$ , and  $\pi/3$  are  $1.88a^2$ ,  $8.0a^2$ , and  $52.3a^2$ , respectively, and from Fig. 4(b) we see that they agree very well with the numerics.

In summary, we studied the GH effect in cold atoms with SO coupling and found that there are two different mechanisms needed for TIR to occur, which can lead to unusual GH shifts, e.g., not only large positive but also large negative GH shifts can be observed. In addition, the modulation of the GH shift can be realized by changing the potential height and the incident energy. Since the GH shift is much larger than the atomic de Broglie wavelength, one can expect that it can be readily measured in experiment from the density evolution of the atomic ensemble via absorption imaging [22].

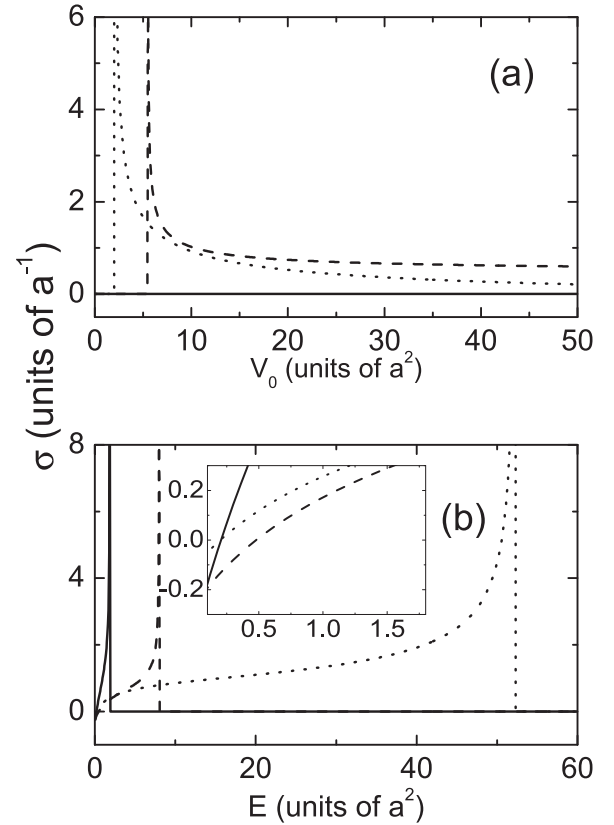


FIG. 4. (a) The GH shift  $\sigma$  vs the potential height  $V_0$  for  $E = 5a^2$  and (b)  $\sigma$  vs the incident energy  $E$  for  $V_0 = 15a^2$  at incident angle  $\varphi = \pi/12$  (solid line),  $\varphi = \pi/6$  (dashed line), and  $\varphi = \pi/3$  (dotted line). The inset figure displays the occurrence of a negative GH shift for a small incident energy.

This work is supported by the National Basic Research Program of China (973 Program) under Grant No. 2011CB921604, and the National Natural Science Foundation

of China under Grants No. 11374003, No. 91436211, No. 11234003, and No. 11129402. Z.L. acknowledges support from EPSRC Grant No. EP/I018514/1.

- 
- [1] F. Goos and H. Hänchen, *Ann. Phys.* **436**, 333 (1947); **440**, 251 (1949).
- [2] C. W. J. Beenakker, R. A. Sepkhanov, A. R. Akhmerov, and J. Tworzydło, *Phys. Rev. Lett.* **102**, 146804 (2009).
- [3] V.-O. de Haan, J. Plomp, T. M. Rekveldt, W. H. Kraan, A. A. van Well, R. M. Dalgliesh, and S. Langridge, *Phys. Rev. Lett.* **104**, 010401 (2010).
- [4] J. Huang, Z. Duan, H. Y. Ling, and W. Zhang, *Phys. Rev. A* **77**, 063608 (2008); Z. Duan, L. Hu, X. Xu, and C. Liu, *Opt. Express* **22**, 17679 (2014).
- [5] For a review, see X. Chen, X.-J. Lu, Y. Ban, and C.-F. Li, *J. Opt.* **15**, 033001 (2013), and references therein.
- [6] D. Dragoman and M. Dragoman, *J. Appl. Phys.* **101**, 104316 (2007).
- [7] X. Chen, J.-W. Tao, and Y. Ban, *Eur. Phys. J. B* **79**, 203 (2011).
- [8] E. Schrödinger, *Sitzungsber. Preuss. Akad. Wiss. Phys. Math. Kl.* **24**, 418 (1930).
- [9] O. Klein, *Z. Phys.* **53**, 157 (1929).
- [10] T. Salger, C. Grossert, S. Kling, and M. Weitz, *Phys. Rev. Lett.* **107**, 240401 (2011).
- [11] L. J. LeBlanc, M. C. Beeler, K. J.-García, A. R. Perry, S. Sugawa, R. A. Williams, and I. B. Spielman, *New J. Phys.* **15**, 073011 (2013).
- [12] D. W. Zhang, Z. D. Wang, and S. L. Zhu, *Front. Phys.* **7**, 31 (2013).
- [13] J. Dalibard, F. Gerbier, G. Juzeliūnas, and P. Öhberg, *Rev. Mod. Phys.* **83**, 1523 (2011); N. Goldman, G. Juzeliūnas, P. Öhberg, I. B. Spielman, *Rep. Prog. Phys.* **77**, 126401 (2014); H. Zhai, *ibid.* **78**, 026001 (2015).
- [14] V. A. Sablikov and Y. Y. Tkach, *Phys. Rev. B* **76**, 245321 (2007).
- [15] Y. Ban and E. Y. Sherman, *Phys. Rev. A* **85**, 052130 (2012).
- [16] Y. Zhang, L. Mao, and C. Zhang, *Phys. Rev. Lett.* **108**, 035302 (2012).
- [17] G. Juzeliūnas, J. Ruseckas, M. Lindberg, L. Santos, and P. Öhberg, *Phys. Rev. A* **77**, 011802(R) (2008).
- [18] C. Zhang, *Phys. Rev. A* **82**, 021607(R) (2010).
- [19] G. Dong, S. Edvardsson, W. Lu, and P. F. Barker, *Phys. Rev. A* **72**, 031605(R) (2005); J. S. Liu and M. R. Taghizadeh, *Opt. Lett.* **27**, 1463 (2002).
- [20] G. Juzeliūnas, J. Ruseckas, A. Jacob, L. Santos, and P. Öhberg, *Phys. Rev. Lett.* **100**, 200405 (2008); G. Juzeliūnas, J. Ruseckas, and J. Dalibard, *Phys. Rev. A* **81**, 053403 (2010).
- [21] In practice, it is not necessary to derive the reflection amplitude when  $V_0 < a^2 + E$  since the reflection amplitude in this case is analytically connected to the one of  $V_0 > a^2 + E$  in the complex plane.
- [22] L. Khaykovich, F. Schreck, G. Ferrari, T. Bourdel, J. Cubizolles, L. D. Carr, Y. Castin, and C. Salomon, *Science* **296**, 1290 (2002).